CHIN. PHYS. LETT. Vol. 33, No. 8 (2016) 085202

A Particle-in-Cell Simulation Study on Harmonic Waves Excited by Electron Beams in Unmagnetized Plasmas *

Jun Guo(郭俊)[1,2]**

[1] College of Mathematics and Physics, Qingdao University of Science and Technology, Qingdao 266061
[2] State Key Laboratory of Space Weather, Chinese Academy of Sciences, Beijing 100190

(Received 30 April 2016)

The excitation of harmonic waves by an electron beam is studied with electrostatic simulations. The results suggest that the harmonic waves are excited during the linear stage of the simulation and are developed in the nonlinear stage. First, the Langmuir waves (LWs) are excited by the beam electrons. Then the coupling of the forward propagating LWs and beam modes will excite the second harmonic waves. The third harmonic waves will be produced if the lower velocity side of the beam still has a positive velocity gradient. The beam velocity decreases at the same time, which provides the energy for wave excitation. We find that it is difficult to excite the harmonic waves with the increase of the thermal velocity of the beam electrons. The beam electrons will be heated after waves are excited, and then the part of the forward propagating LWs will turn into electron acoustic waves under the condition with a large enough intensity of beam electrons. Moreover, the action of ions hardly affects the formation of harmonic waves.

PACS: 52.35.Qz, 52.35.Fp, 52.65.Rr DOI: 10.1088/0256-307X/33/8/085202

The electron beam is always considered to be related to the generation of electrostatic waves.[1–4] For example, the Langmuir waves (LWs), which are often observed in the Earth's electron foreshock,[5] can be generated by electron beams. Moreover, harmonic waves with frequencies of about several times of the local plasma frequency $\omega_{\rm pe}$ can also be excited by the electron beam.[6] The previous studies[7] show that the electron higher order modes may play a physically significant role in a plasma which is composed of two electron species. The observational results also suggest that the second and third harmonic plasma waves can be found not only in the vicinity of the Earth's bow shock[8,9] but also during solar type Ⅱ and occasionally found during type Ⅲ radio bursts.[10,11] The excitation mechanism of harmonic waves has been discussed for many years. There are two kinds of harmonic waves, electrostatic and electromagnetic waves at $2\omega_{\rm pe}$. There is today general agreement that the second electromagnetic harmonic waves at $2\omega_{\rm pe}$ are produced through coalescence of the forward and backward propagating LWs.[12,13] However, the excitation mechanism of the electrostatic harmonic waves is still an open problem. Klimas[14] suggested that the mechanism for excitation of the electrostatic second harmonic $2\omega_{\rm pe}$ waves is due to second-order wave–wave coupling of the forward propagating LWs, which takes place during the nonlinear stage of the simulations. In their simulation, the dominant unstable mode which continually grows pumps field modes decaying in the earlier time. Then the oscillation frequencies of these pumped modes will suddenly shift to harmonic frequencies of the unstable mode. Nishikawa *et al.*[15] also found that the pumping waves and beam density significantly affect the levels of harmonic waves. However, the high levels of harmonic waves were not found in their simulation. Under different conditions with two electron components of different temperatures, Schriver *et al.*[16] found the electron acoustic instability associated with the excitation of electrostatic $2\omega_{\rm pe}$ waves. They suggested that it is wave coupling between waves along the electron acoustic branch which generates waves with frequencies just below $2\omega_{\rm pe}$. Yoon *et al.*[17] proposed that an energetic electron beam modulated by intense backward propagating LWs is associated with the electrostatic $2\omega_{\rm pe}$ wave. Using a particle-in-cell simulation, Sauer *et al.*[18] investigated the Langmuir oscillations in the plasma with plateau distributions. They suggested that the Langmuir oscillations at $k = 0$ and $\omega = 2\omega_{\rm pe}$ and the beam instability are contributed to the second harmonic waves. They also found that the backward propagating LW is independent of any electrostatic harmonic waves. However, they did not study the second harmonic generation in their work.

In this Letter, one-dimensional particle-in-cell simulation is carried out to investigate the excitation of harmonic waves in an unmagnetized plasma, which consists of two components: background and beam electrons. We discuss the harmonic waves under different initial conditions, and describe the simulation code and parameters. The simulation results are also presented.

We have performed one-dimensional electrostatic particle simulation. In our simulation, $n_{\rm b}$ represents the unperturbed density of the beam electron, and n_0 is the total electron density. Here $V_{\rm theb}$ and $u_{\rm d}$ denote the thermal velocity and drifting speed of beam

*Supported by the National Natural Science Foundation of China under Grant No 41204115, and the Specialized Research Fund for State Key Laboratories.

**Corresponding author. Email: guojun@qust.edu.cn

© 2016 Chinese Physical Society and IOP Publishing Ltd

electrons, respectively. The time is normalized by the inverse of the electron plasma frequency $\omega_{\rm pe}$, and the velocity is normalized by the initial background electron thermal velocity $v_{\rm the}$, thus the distance is normalized by the electron Debye length $\lambda_{\rm De}$. The simulation is carried out in the region with length $L = 2048\lambda_{\rm De}$. The 8192 grid system is employed, and the spatial resolution is $\Delta x = 0.25\lambda_{\rm De}$. The time step is $t = 0.01\omega_{\rm pe}^{-1}$. Initially, velocity distributions of the beam and background electron are Maxwellian, and the ions are motionless and form a neutralizing background except for the last run. The number of each species in a cell is 100, which is close to that used in previous simulations.[19,20] The typical relative beam densities used in the simulation of the foreshock waves is about from 10^{-3} to 0.05.[14] We have performed a total of five cases. The parameters are listed in Table 1.

Table 1. Initial plasma parameters for five runs.

Run	$v_{\rm theb}/v_{\rm the}$	$n_{\rm b}/n_0$	$u_{\rm d}/v_{\rm the}$	$m_{\rm i}/m_{\rm e}$
1	1	0.1	10	∞
2	1	0.1	5	∞
3	1	0.5	5	∞
4	5	0.5	5	∞
5	1	0.5	5	1836

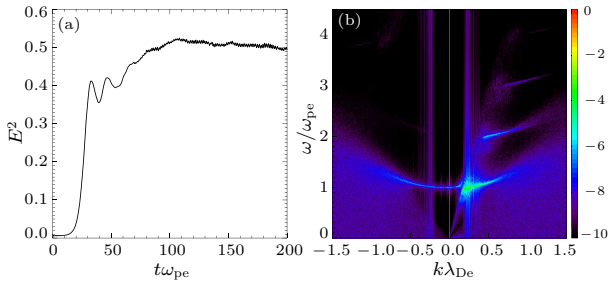

Fig. 1. (a) The normalized wave energy versus the time for run 1. (b) The ω–k diagram obtained by the Fourier transformation of the electric field.

Figure 1(a) is the normalized wave energy versus time for run 1. In Fig. 1(a), the time period $\omega_{\rm pe}t \sim 0$–33 corresponds to the linear growth stages. The ω–k diagram obtained by the Fourier transformation of the electric field is shown in Fig. 1(b). The power spectrum in Fig. 1(b) is calculated by the electric field data from $\omega_{\rm pe}t = 0$ to 409.6 and all of the simulation grids. Figure 1(b) shows the presence of the forward and backward Langmuir waves, the second and third harmonic waves. The amplitude of the third harmonic waves is much less than that of the second harmonic waves. We should note that the starting point of the wave number of the third harmonic waves is larger than that of the second harmonic waves.

The evolution detail of electrostatic waves is illustrated in Figs. 2(a) $\omega_{\rm pe}t = 0$–10.24, 2(b) $\omega_{\rm pe}t = 14$–24.24, and 2(c) $\omega_{\rm pe}t = 20.49$–30.72. The solid black curve represents the theoretical dispersion relation of LWs based on initial parameters. The beam density is much smaller in this run, $n_{\rm b} \ll n_0$, thus the electrostatic waves driven by the beam electron can be regarded as the beam-driven wave mode whose dispersion relation can be expressed with $\omega \approx ku_{\rm d}$.[21,22] The red curve just represents the theoretical dispersion relation of beam modes. At the first period shown in Fig. 2(a), only LWs can be found. As time proceeds, Fig. 2(b) shows that the amplitude at the point $\omega/\omega_{\rm pe} \sim 1.0$ and $k\lambda_{\rm De} \sim 0.1$ increases. This point is only the intersection that two dispersion relation curves cross. Now the beam streaming speed is reduced to $u_{\rm d} \sim 9.0v_{\rm the}$. Moreover, the relatively weak waves appear at $\omega/\omega_{\rm pe} \sim 1.8$ and $k\lambda_{\rm De} \sim 0.2$, which means that the weak second harmonic waves appear. In Fig. 2(c), the amplitude at the point $\omega/\omega_{\rm pe} \sim 1.0$ and $k\lambda_{\rm De} \sim 0.1$ continues to increase. In particular, the third harmonic waves appear, and intensity of the second harmonic waves continues to increase during this period. At the same time, the beam streaming speed is reduced to $u_{\rm d} \sim 8.7v_{\rm the}$. The process be concluded as follows: (1) The coupling of the forward LWs and beam-driven waves excites the second harmonic waves. (2) The second waves couple with beam-driven instabilities, exciting the third harmonic waves. The decrease of the streaming speed of the electron beam can explain the feature shown in Fig. 1(b): the starting point of the wave number of the third harmonic waves is larger than that of the second harmonic waves. Figure 2 mainly corresponds to the linear growth stage, which suggests that the couple of LWs and beam mode excites the harmonic waves during the linear period. Our conclusion is very different from previous results,[14,16] that is, the harmonic waves are excited during the nonlinear stage. On the other hand, Huang *et al.*[19] also found that the second harmonic LWs are mainly derived from the contribution of the beam electrons, which is consistent with our results. However, they did not give the evolution details of the harmonic waves during the linear period.

Figure 3(a) is the ω–k diagram at $\omega_{\rm pe}t = 0$–409.6 for run 2 with $v_{\rm theb}/v_{\rm the} = 5$. Only the initial drift velocity of the beam electron differs from that of run 1. It is obvious that the amplitude of the second harmonic wave is very small, which is much less than that in Fig. 1(b). Also, no third harmonic waves are produced. Compared with the results shown in Fig. 1(b), the starting point of the wave number of the second harmonic waves in this figure is larger than that of run 1 due to the small drift velocity of the beam electron. The frequency $\omega/\omega_{\rm pe}$ ranges from 2.0 to 2.2. It has been reported that the electron acoustic mode may be excited in a plasma containing two electron components with different temperatures.[23] The red solid line is the dispersion relation for electron acoustic waves, $\omega^2 = \omega_{\rm pc}^2(1 + 3k^2\lambda_{\rm Dc}^2)/(1 + 1/(k^2\lambda_{\rm Dh}^2))$, where $\omega_{\rm pc}$ is the cool electron plasma waves, $\lambda_{\rm Dc}$ and $\lambda_{\rm Dh}$ are cool and hot electron Debye lengths, respectively. In our simulation, the beam electrons will be heated and can be regarded as the hot electrons, then the background electrons can be regarded as cool electrons. In the figure, only the LWs are obvious in this region

with $k\lambda_{De} < 0.3$. The forward propagating LWs are strongly damped and electron acoustic waves are the dominant waves in the region with $k\lambda_{De} > 0.3$. Figure 3(b) is the ω–k diagram for run 3. In this run, the density of beam electron increases. Compared with the results shown in Fig. 3(a), the forward propagating electron acoustic waves become intense due to the larger number of hot electrons. With the increase of the beam density, the dominant frequency of the electron acoustic waves decreases, which leads to the frequency reduction of the harmonic waves. Its frequency ω/ω_{pe} ranges from 1.8 to 2.1. The beam modes with $k\lambda_{De} < 0.3$ are weakly damped compared with the result shown in Fig. 3(a). The forward propagating LWs with the Doppler-shifted frequency developed in the direction of higher frequency. Their maximum frequency ω/ω_{pe} of LWs is about 1.3, which is larger than that in Fig. 3(a) (ω/ω_{pe} is about 1.1). All of the above suggest that the harmonic waves are produced by the coupling of the LWs and beam modes. When the beam electrons are heated, part of the forward propagating LWs will turn into the electron acoustic waves.

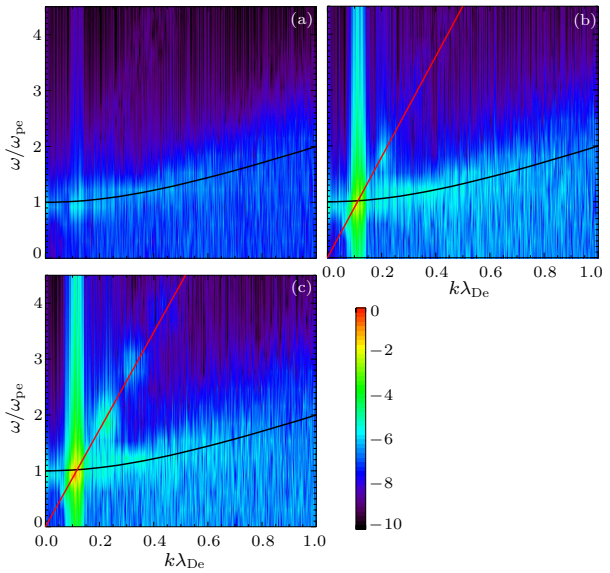

Fig. 2. The evolution detail of electrostatic waves for run 1: (a) $\omega_{pe}t$ =0–10.24, (b) $\omega_{pe}t$ = 14–24.24, and (c) $\omega_{pe}t$ = 20.49–30.72. The solid black curve represents the theoretical dispersion relation of LWs based on initial parameters. The red curve represents the theoretical dispersion relation of beam modes.

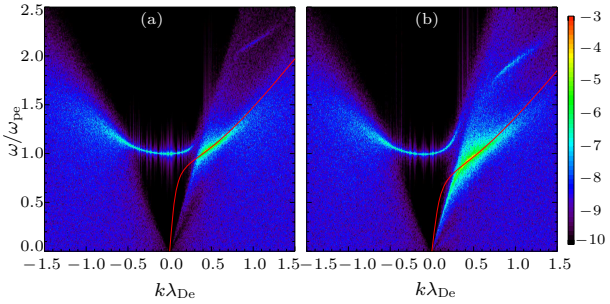

Fig. 3. The ω–k diagrams obtained by the Fourier transformation of the electric field for runs (a) 2 and (b) 3.

However, if the beam thermal velocity increases, $v_{theb}/v_{the} = 5$ is used for run 4, no harmonic waves appear during the simulation. That is, the beam thermal velocity has an important effect on the harmonic waves. For the power spectrum shown in Fig. 4, we use data taken from $\omega_{pe}t = 0$ to 409.6. We can find that the harmonic wave is not generated. Figure 5 shows the velocity distributions of electrons in runs 1, 2 and 4, respectively. For run 1, black, blue and red curves give the distributions at $\omega_{pe}t = 0$, 20 and 30, which are corresponding to Fig. 2. Obviously, every velocity distribution function for run 1 has a positive slope at the speed smaller than the beam drift speed. At the same time, the beam is decelerated and heated. For runs 2 and 4, the black and red curves give the forms at $\omega_{pe}t = 0$ and 400, respectively. The positive slope disappears, which can explain the weak harmonic waves shown in Fig. 3(a). However, the velocity distribution basically stays the same and the positive slope can hardly be seen in run 4. In a word, a distribution with a positive slope will be unstable, which leads to the coupling between the beam mode and the LWs. The energy stored in the beam promotes the development of the instabilities.

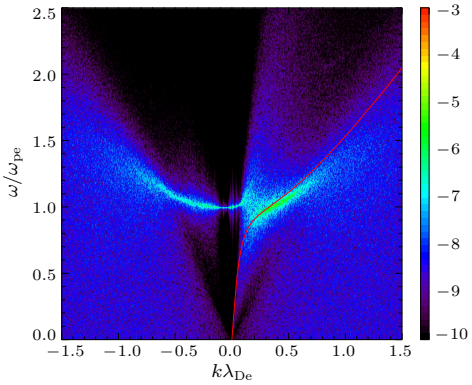

Fig. 4. The ω–k diagram for run 4 from $\omega_{pe}t = 0$ to 409.6.

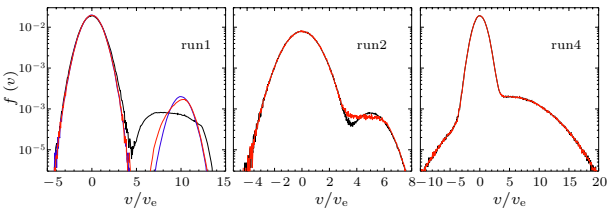

Fig. 5. The velocity distributions of electron in runs 1 and 4, respectively. For run 1, the black, blue and red curves give the forms at $\omega_{pe}t = 0$, 20 and 30. For runs 2 and 4, the black and red curves give the forms at $\omega_{pe}t = 0$ and 400, respectively.

The previous work[19] suggests that ions play a key role in exciting the backward propagating LWs. The electron beam may directly amplify the second harmonic waves. Then the ions are considered and $m_i/m_e = 1836$, $T_i/T_e = 4$, the other conditions are the same as those in run 3. The dispersion diagram is shown in Fig. 6 for run 5. Compared with that in Fig. 3(b), the ion-acoustic waves appear. More-

over, the frequency width of LWs becomes broader and amplitude obviously becomes intense. The maximum of the electron acoustic waves slightly decreases, and this hardly affects the amplitude of second harmonic waves. Our simulation results confirm that the backward propagating LWs do not directly affect the formation of the harmonic waves.

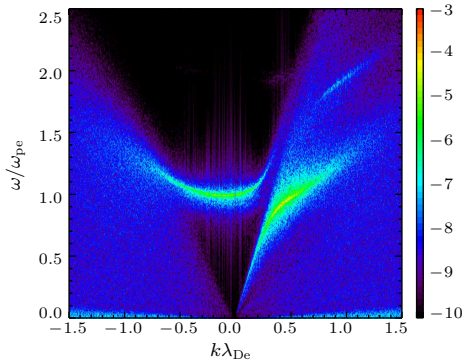

Fig. 6. The ω–k diagram at $\omega_{pe}t = 0$–409.6 for run 5 with $m_i/m_e = 1836$, and the other conditions are the same as those in run 3.

In summary, the harmonic waves excited by electron beams are studied with 1D electrostatic simulation. The effects of the drift velocity, temperature and density of electron beams are used in these simulations. Our simulation results suggest that the harmonic waves will be excited in the linear stage and will be developed in the nonlinear stage if the positive slope of electron distribution exists. The main processes are concluded as follows: (1) The LWs are excited by the beam electrons first. (2) The second harmonic waves are excited by the coupling of the forward propagating LWs and beam modes, and the beam velocity decreases at the same time. (3) As things progress, the intensity of the coupling point continues to increase. The third harmonic waves will be excited if the lower velocity side of the beam still has a positive velocity gradient. (4) When the thermal velocity of the beam electrons increases, the positive velocity gradient of the distribution begins to disappear gradually. Then the electron beam hardly excites the harmonic waves. (5) After waves are excited, some electrons are heated, then parts of the forward propagating LWs will turn into electron acoustic waves, which is from the coupling point toward the large wave number. (6) The action of ions is disturbed, the frequency band of LWs is broadened, and the amplitude of LWs increases. The results suggest that the ion can hardly affect the formation of harmonic waves.

References

[1] Lu Q M, Lembege B, Tao J B and Wang S 2008 *J. Geophys. Res.* **113** A11219
[2] Wu M Y, Lu Q M, Zhu J, Du A M and Wang S 2012 *Astrophys. Space Sci.* **338** 81
[3] Wu M Y, Lu Q M, Zhu J, Wang R S and Wang S 2013 *Plasma Sci. Technol.* **15** 17
[4] Guo J and Yu B 2012 *Chin. Phys. Lett.* **29** 035203
[5] Anderson R R, Eastman T E, Gurnett D A, Frank L A and Parks G K 1981 *J. Geophys. Res.* **86** 4493
[6] Thomsen M F, Gary S P, Feldman W C, Cole T E and Barr H C 1983 *J. Geophys. Res.* **88** 3035
[7] Mace R L and Hellberg M A 1990 *J. Plasma Phys.* **43** 239
[8] Cairns I H 1986 *J. Geophys. Res.* **91** 2975
[9] Treumann R A, Bauer O H, LaBelle J, Haerendel G, Christiansen P J, Darbyshire A G, Norris A J, Woolliscroft L J C, Anderson R R, Gurnett D A, Holtzworth R W, Koons H C and Roeder J 1986 *Adv. Space Res.* **6** 93
[10] Kliem B, Krüger A and Treumann R A 1992 *Sol. Phys.* **140** 149
[11] Thejappa G and MacDowall R J 2014 *ASP Conf. Ser.* (Myrtle Beach South Carolina 14-19 April 2013) **484** p210
[12] Cairns Iver H and Robinson P A 1995 *Geophys. Res. Lett.* **22** 3437
[13] Kasaba Y, Matsumoto H and Omura Y 2001 *J. Geophys. Res.* **106** 18693
[14] Klimass A J 1983 *J. Geophys. Res.* **88** 9081
[15] Nishikawa K I and Cairns I H 1991 *J. Geophys. Res.* **96** 19343
[16] Schriver D, Ashour-Abdalla M, Sotnikov V, Hellinger P, Fiala V, Bingham R and Mangeney A 2000 *J. Geophys. Res.* **105** 12919
[17] Yoon P H, Wu C S, Vinus A F, Reiner M J, Fainberg J and Stone R G 1994 *J. Geophys. Res.* **99** 23481
[18] Sauer K and Sydora R D 2015 *J. Geophys. Res.* **120** 235
[19] Huang Y and Huang G L 2009 *Astron. Astrophys.* **503** 207
[20] Huang Y and Huang G L 2008 *Adv. Space Res.* **41** 1202
[21] Lu Q M, Wang S and Dou X K 2005 *Phys. Plasmas* **12** 072903
[22] Treumann R and Baumjohann W 1997 *Advanced Space Plasma Physics* (London: Imperial College Press) chap 4 p 73
[23] Gary S P and Tokar R L 1985 *Phys. Fluids* **28** 2439